

# Robust Adaptive Tracking Control for Uncertain Five-Bar Parallel Robot Using Fuzzy CMAC in Order to Improve Accuracy

Thanh Quyen Ngo <sup>1\*</sup>, Thanh Hai Tran <sup>2</sup>, Tong Tan Hoa Le <sup>3</sup>

<sup>1,3</sup> Faculty of Electrical Engineering Technology, Industrial University of Ho Chi Minh City, Vietnam

<sup>2</sup> Office of Planning and Investment, Industrial University of Ho Chi Minh City, Vietnam

Email: <sup>1</sup> ngothanquyen@iuh.edu.vn, <sup>2</sup> tranthanhhai@iuh.edu.vn, <sup>3</sup> letongtanhoa@iuh.edu.vn

\*Corresponding Author

**Abstract**—Parallel robot systems are increasingly important and widely applied due to their superior advantages such as high speed and accuracy. To improve the accuracy of these systems, recent research has focused on developing advanced control methods. However, this remains a significant challenge due to the complex mathematical model of parallel robots. This study introduces a control system based on a fuzzy cerebellar model articulation controller (FCMAC) to control parallel robots. The proposed control system includes FCMAC as the main tracking controller used to estimate the ideal control. A robust controller is employed to compensate for the error between FCMAC and the ideal controller. The parameters of FCMAC are adjusted online based on adaptive laws derived from Lyapunov functions. Finally, a five-bar parallel robot is selected to experiment with the FCMAC algorithm to demonstrate the effectiveness of the proposed controller. The results show that the accuracy of FCMAC is better than that of other algorithms.

**Keywords**—Cerebellar Model Articulation Controller; Adaptive Control; Fuzzy; Fuzzy Cerebellar Model Articulation Controller; Five-Bar Parallel Robot.

## I. INTRODUCTION

In recent years, there has been a growing interest in dynamic control systems like robots [1]–[8]. However, traditional control methods such as PID controllers and sliding mode control often fall short when dealing with complex nonlinear systems that are multi-variable. On the other hand, model-based controllers tend to be more accurate than model-free ones, especially when the system has an accurate dynamic model [9]–[21]. Yet, achieving this accuracy is challenging due to uncertainties like model errors, parameter disturbances, and deviations from the intended trajectory. To address these uncertainties, various methods have been developed, including adaptive controllers [9]–[10], model predictive controllers [11]–[13], robust controllers [14]–[17], Lyapunov-based controllers [18]–[19], and sliding mode controllers [20]–[21]. While all these methods aim for high accuracy, they still grapple with uncertainty during system operation, highlighting the need for further research to enhance controller quality for nonlinear systems.

Combining the sliding control structure with neural networks has emerged as a potential way to boost robot performance [22]–[26]. However, achieving precise and reliable models presents significant challenges, often resulting in less-than-desirable precision [27]. To overcome

this hurdle, researchers have turned to artificial neural networks (ANNs) to compensate for uncertainties in mathematical models, aiming to mimic ideal sliding mode control (SMC) systems [28]. These efforts address the significant challenge posed by uncertain and nonlinear system components, particularly when conventional methods struggle.

Using Artificial Neural Networks (ANN) in robot motion control poses two significant challenges. Firstly, ANN in robot controllers must ensure sufficient nonlinear learning capability to approximate ideal controllers effectively through online learning rules. An efficient method is to employ the Cerebellar Model Articulation Controller (CMAC), which is widely applied in various applications due to its fast learning ability and simple structure [29]–[30]. CMAC not only adapts quickly but also mitigates unwarranted drawbacks [31]. However, these studies often focus solely on capturing errors from the output of neural network-based controllers to assess the learning process and update network weights. This may limit the evaluation of the robot's quality during parameter adjustment.

The second challenge in using ANN is ensuring it contains enough adjustable parameters to eliminate the system's uncertain components. Facing this issue, studies in intelligent control have proposed methods directly integrating human expertise into neural networks [32]–[37]. Recently, fuzzy inference systems have been successfully applied as adaptive controllers for robots [38]–[42], one of the most successful applications of fuzzy logic systems [43]–[46]. The flexibility of fuzzy controllers helps address uncertain system components, enabling the robot's adaptive behavior in dynamic environments. Although neural networks have been developed in various ways to cope with uncertain components [47]–[51], the limitations of adjustable parameters may lead to decreased controller accuracy [52].

In recent years, the CMAC control model has demonstrated its ability to achieve fast convergence and good generalization in identifying and controlling complex dynamic systems [53]. The structure of CMAC is built from a network of associative memories with partially connected input fields and overlapping spaces. It has been proven that CMAC can approximate a nonlinear function with any degree of accuracy [54]. Gradient descent algorithms, like



backpropagation (BP), are used to minimize approximation errors by searching for the parameter weights of the network model [55]–[56]. BP is considered a fundamental method for training CMAC models in control system applications. However, the main drawbacks of BP are its slow convergence rate and inability to achieve global minima [57].

To address the limitations of CMAC, research [58] has combined it with fuzzy logic to create a fuzzy cerebellar model articulation controller (FCMAC). In another study, [59] simulated the system model using FCMAC to create a robust controller for a robot controller. To identify the dynamic model of a fractional-order chaotic system, research [60] designed a Type-2 FCMAC. Several other studies related to FCMAC can be found in [61]. FCMAC has extraordinary capabilities in controlling and improving system accuracy. Therefore, it has been used to control uncertain components of nonlinear systems. Subsequently, an adaptive robust controller is proposed to enhance the control system's quality. The combination of CMAC and fuzzy logic in FCMAC provides a flexible network structure with good adaptability in multivariable environments. This increases accuracy and adaptability to challenges in controlling robots and other complex dynamic systems.

This paper contributes significantly in three main aspects:

- Firstly, it employs the Fuzzy Cerebellar Model Articulation Controller (FCMAC) to estimate uncertain components, thereby enhancing control capability and adaptability to uncertain factors.
- Secondly, it introduces an additional robust controller coordinated with FCMAC to achieve high accuracy in the control process.
- Lastly, the paper provides theoretical analysis and conducts experiments to validate the proposed controller, enabling the evaluation of its accuracy and effectiveness under actual conditions.

The article is structured as follows: Part 2 presents the detailed mathematical model of the five-bar parallel robot. Then, in Section 3, the FCMAC model theory is introduced. Part 4 delves into the robot's control system and demonstrates how to analyze stability using Lyapunov. The process of testing the FCMAC algorithm is presented in Part 5. At the end of the article, Part 6 summarizes and draws conclusions based on the information presented.

## II. DYNAMIC EQUATION DESCRIPTION

The dynamics of a five-bar parallel robot system expressed in the Lagrange following form:

$$M'(q')\ddot{q}' + C'(q', \dot{q}')\dot{q}' + g'(q') = \tau \quad (1)$$

Where  $q' = (q_1, q_2, q_3, q_4)^T$  represents the robot's general coordinates.  $q', \dot{q}, \ddot{q} \in R^{4 \times 1}$  are the position, velocity, and joint acceleration vectors;  $M'(q') \in R^{4 \times 4}$  is the moment of inertia matrix;  $C'(q', \dot{q}') \in R^{4 \times 4}$  are the centripetal force and the Coriolis force;  $g'(q') \in R^{4 \times 1}$  is the gravity vector;  $\tau$  is the control variable. This study uses a robot model with five-bar parallel, as shown in Fig. 1, to evaluate the kinematic characteristics. The relationship between  $q_3$  and  $q_4$  expressed based on  $q_1$  and  $q_2$  is expressed as Eq. (2) and (3).

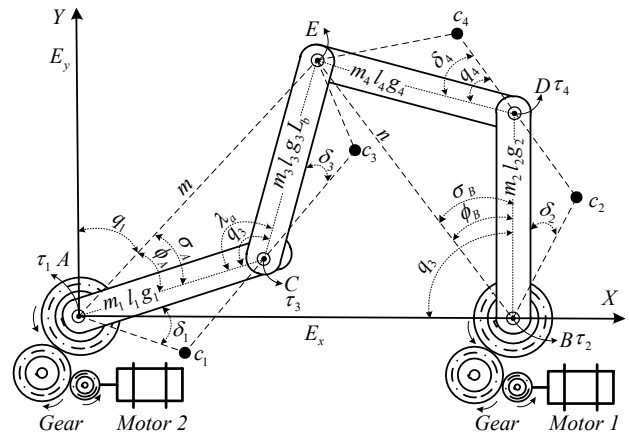


Fig. 1. Structure diagram of five-bar parallel robot

$$q_4 = \arctan \left[ \frac{\pm \sqrt{\mathcal{A}^2(q_1, q_2) + \mathcal{B}^2(q_1, q_2) - \mathcal{C}^2(q_1, q_2)}}{\mathcal{C}(q_1, q_2)} \right] + \arctan \left[ \frac{\mathcal{B}(q_1, q_2)}{\mathcal{A}(q_1, q_2)} \right] - q_2 \quad (2)$$

$$q_3 = \arctan \left[ \frac{\mu(q_1, q_2) + l_4 \sin(q_2 + q_4)}{\lambda(q_1, q_2) + l_4 \sin(q_2 + q_4)} \right] - q_1 \quad (3)$$

$$\mathcal{A}(q_1, q_2) = 2l_4 \lambda(q_1, q_2)$$

$$\mathcal{B}(q_1, q_2) = 2l_4 \mu(q_1, q_2)$$

$$\mathcal{C}(q_1, q_2) = l_3^2 - l_4^2 - \lambda^2(q_1, q_2) - \mu^2(q_1, q_2)$$

$$\lambda(q_1, q_2) = l_2 \cos(q_2) - l_1 \cos(q_1) + l_5$$

$$\mu(q_1, q_2) = l_2 \sin(q_2) - l_1 \sin(q_1)$$

Moment of inertia matrix:

$$M'(q') = \begin{bmatrix} m'_{11} & 0 & m'_{13} & 0 \\ 0 & m'_{22} & 0 & m'_{24} \\ m'_{31} & 0 & m'_{33} & 0 \\ 0 & m'_{42} & 0 & m'_{44} \end{bmatrix} \quad (4)$$

$$m'_{11} = m_1 \tau_1^2 + m_3 (l_1^2 + \tau_3^2 + l_1 \tau_3 \cos(q_3 + \delta_3)) + J_1 + J_3$$

$$m'_{13} = m_3 (\tau_3^2 + l_1 \tau_3 \cos(q_3 + \delta_3)) + J_3$$

$$m'_{31} = m'_{13}$$

$$m'_{22} = m_2 \tau_2^2 + m_4 (\tau_2^2 + \tau_4^2 + l_2 \tau_4 \cos(q_4 + \delta_4)) + J_2 + J_4$$

$$m'_{24} = m_4 (\tau_2^2 + l_2 \tau_4 \cos(q_4 + \delta_4)) + J_4$$

$$m'_{42} = m'_{24}$$

$$m'_{33} = m_3 \tau_3^2 + J_3$$

$$m'_{44} = m_4 \tau_4^2 + J_4$$

Centripetal force is expressed as:

$$C'(q', \dot{q}') = \begin{bmatrix} \gamma_1 \dot{q}_3 & 0 & \gamma_1 (\dot{q}_1 + \dot{q}_3) & 0 \\ 0 & \gamma_2 \dot{q}_4 & 0 & \gamma_2 (\dot{q}_2 + \dot{q}_4) \\ -\gamma_1 \dot{q}_1 & 0 & 0 & 0 \\ 0 & -\gamma_2 \dot{q}_2 & 0 & 0 \end{bmatrix} \quad (5)$$

$$\gamma_1 = -m_3 l_1 \tau_3 \sin(q_3 + \delta_3)$$

$$\gamma_2 = -m_4 l_2 \tau_4 \sin(q_4 + \delta_4)$$

Gravity matrix (6).

$$g'(q') = 9.81 \times \begin{bmatrix} g_1 \\ g_2 \\ g_3 \\ g_4 \end{bmatrix} \quad (6)$$

$$g'_1 = (m_1\tau_1 + m_3l_1)\cos(q_1 + \delta_1) + m_3\tau_3\cos(q_1 + q_3 + \delta_3)$$

$$g'_2 = (m_2\tau_2 + m_4l_2)\cos(q_2 + \delta_2) + m_4\tau_4\cos(q_2 + q_4 + \delta_3)$$

$$g'_3 = m_3\tau_3\cos(q_1 + q_3 + \delta_3)$$

$$g'_4 = m_4\tau_4\cos(q_2 + q_4 + \delta_4)$$

However, the five-bar parallel robot system has only two control positions, represented by  $q = (q_1, q_2)^T$ . The relationship between  $q$  and  $q'$  can be deduced as follows:

$$q = \begin{bmatrix} 1 & 0 & 0 & 0 \\ 0 & 1 & 0 & 0 \end{bmatrix} q' = \alpha(q') \quad (7)$$

$$q' = \sigma(q) \quad (8)$$

Based on equations (7), (8), the system's dynamic model is determined in [62]:

$$M(q')\ddot{q} + C(q', \dot{q}')\dot{q} + B_m\dot{q} + g(q') = \tau \quad (9)$$

$$\dot{q}' = \rho(q')\dot{q} \quad (10)$$

$$q' = \sigma(q) \quad (11)$$

Here,  $B_m = (b_{m1}, b_{m2})$  represents the viscosity of the motor in the system. The system has only two control input values denoted  $\tau = [\tau_1, \tau_2]^T$ . The components of the matrix in equation (9) are calculated as follows:  $M(q') = \rho^T(q')M'(q')\rho(q')$ ;  $C(q', \dot{q}') = \rho^T(q')C'(q')\rho(q')$ ;  $g(q') = \rho^T(q')g'(q')$ .

In the nonlinear system, the state vector equation of the robot arm system is expressed:

$$\ddot{q}(t) = -\frac{C(q', \dot{q}')\dot{q} + B_m\dot{q} + g(q')}{M(q')} + \frac{K_\tau I_m}{M(q')} = f(\underline{x}, t) + g(\underline{x}, t)K_\tau I_m \quad (12)$$

In which,  $f(\underline{x}, t) = -\frac{C(q', \dot{q}')\dot{q} + B_m\dot{q} + g(q')}{M(q')}$  and  $g(\underline{x}, t) = \frac{1}{M(q')}$  are nonlinear dynamic functions that are difficult to determine. Therefore, it is impractical to design a controller based on an exact mathematical model of the object. For example, if the actual values of  $f(\underline{x}, t)$ ,  $g(\underline{x}, t)$  were known exactly and were denoted by  $F_0(\underline{x}, t)$ ,  $G_0(\underline{x}, t)$  respectively. Where  $F_0(\underline{x}, t)$ ,  $G_0(\underline{x}, t)$  are nominal components that do not change and  $L(\underline{x}, t)$  is defined as the sum of the Uncertain components exist in the system. The state vector  $\underline{x}(t) = [x^T \ \dot{x}^T \ \dots \ x^{(n-1)T}]^T$  are the components of the state vector of the joint. Therefore, equation (12) is rewritten as follows:

$$\ddot{q}(t) = F_0(\underline{x}, t) + G_0(\underline{x}, t) + L(\underline{x}, t) \quad (13)$$

Control in nonlinear systems poses an important challenge. The error  $e(t) \in R^{n \times 1}$  must be continuously monitored, defined by subtracting the desired value  $q_d(t)$  from the actual value of the system  $q(t)$ . The system's tracking error is described as follows:

$$e(t) = q_d(t) - q(t) \quad (14)$$

The tracking error of the system is represented in vector form as follows:

$$\underline{e}(t) = [e^T \ \dot{e}^T, \dots, \ e^{(n-1)T}]^T \quad (15)$$

The sliding surface is defined as:

$$s(\underline{e}(t)) = e^{(n-1)}(t) + \zeta_1 e^{(n-2)}(t) + \dots + \zeta_{n-1} e(t) + \zeta_n \int_0^t e(t) dt \quad (16)$$

Here,  $s = [s_1 \ s_2 \ \dots \ s_k]^T$  and  $\zeta_i = \text{diag}(\zeta_{i1}, \zeta_{i2}, \dots, \zeta_{ik})$  with  $i = 1, 2, 3, \dots, n$ . The  $\zeta_i$  is assumed to satisfy the Hurwitz polynomial. Differentiating  $s(\underline{e}(t))$  with respect to time and applying (9) leads to:

$$\dot{s}(\underline{e}(t)) = \ddot{q} - M^{-1}[\tau - C\dot{q} - B_m\dot{q} - g] + K^T \underline{e}(t) \quad (17)$$

Where  $K = [\zeta_n \ \zeta_{n-1} \ \dots \ \zeta_1]^T$  denotes the feedback gain matrix. If assume that the components  $F_0(\underline{x}, t)$ ,  $G_0(\underline{x}, t)$  and the sum of the unknown components  $L(\underline{x}, t)$  has been determined, then the ideal controller can be designed as follows:

$$\tau_{IDEAL} = G_0^{-1} [\ddot{q}_d - F_0(\underline{x}) - L(\underline{x}) + K^T \underline{e} + \rho \text{sgn}[s(\underline{e}(t))]] \quad (18)$$

Where  $\rho \text{sgn}[s(\underline{e}(t))]$  represents the learning law of the sliding surface generator and  $\rho > 0$ . However, the problem is that it is impossible to accurately determine the parameters of the component  $L(\underline{x}, t)$ . Therefore, the study proposes a control system described in detail in section 4.

$$\tau_{controller} = \tau_{FCMAC} + \tau_{RC} = \widehat{W}^T T + \tau_{RC} \quad (19)$$

In this control structure,  $\tau_{FCMAC}$  is the main controller to approximate the ideal controller. The goal is to keep  $\tau_{FCMAC}$  as close as possible to  $\tau_{IDEAL}$ . Besides, to compensate for the appearing approximation errors, a robust controller  $\tau_{RC}$  is incorporated. This way,  $\tau_{RC}$  helps maintain system stability and adaptability, ensuring peripheral errors do not affect control performance.

### III. CONTROLLERS

#### A. Definition of FCMAC controller

FCMAC is a rule class presented as follows:

$$R^l: \text{if } X_1 \text{ is } \mu_{1jk} \text{ and } X_2 \text{ is } \mu_{2jk}, \dots, X_{n_i} \text{ is } \mu_{i j k} \text{ then } O_{jk} = w_{jk} \quad (20)$$

$$\text{For } i = 1, 2, \dots, n_i, \ j = 1, 2, \dots, n_j, \ k = 1, 2, \dots, n_k \text{ and } l = 1, 2, \dots, n_k n_j$$

Here,  $n_i$  refers to the number of input dimensions,  $n_j$  is the number of layers for each input dimension,  $n_k$  is the number of blocks for each layer,  $l = n_k n_j$  is a number of fuzzy rules, and  $\mu_{ijk}$  is the fuzzy set corresponding to the  $i$ th input, the  $j$ th layer, and the  $k$ th block.  $w_{jk}$  represents the output weight of the consequence part.

Fig. 2 describes the FCMAC network structure including Input space, Association memory space, Receptive-field space, Weight memory space, Output space. Details of the classes are described as follows:

1) *Input space S*: It is a continuous multidimensional input space. For each value  $S = [s_1, s_2]^T \in R^n$ , each input state variable  $s_i$  needs to be divided into separate, defined elements in the given space.

2) *Association Memory Space A*: Several elements can be accumulated to form a block. In this space, each block implements a receptive basis function. In this case, the Gaussian function is often used as the admittance basis function and can be expressed and depicted in Fig. 3.

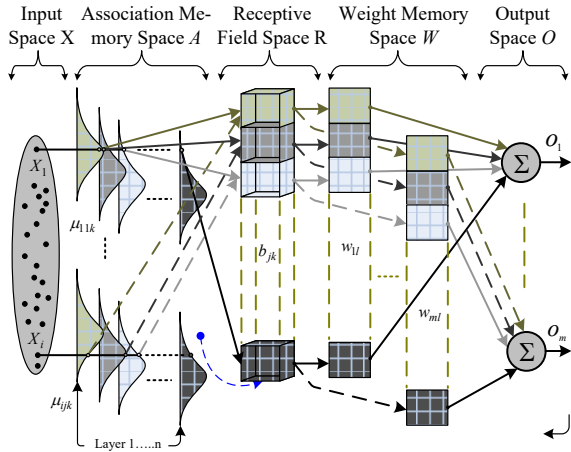


Fig. 2. Architecture of a FCMAC

$$\mu_{ijk}(s_i) = \exp \left[ \frac{-(s_i - m_{ijk})^2}{\sigma_{ijk}^2} \right] \quad (21)$$

Where  $m_{ijk}$  is a translation parameter and  $\sigma_{ijk}$  is dilation.

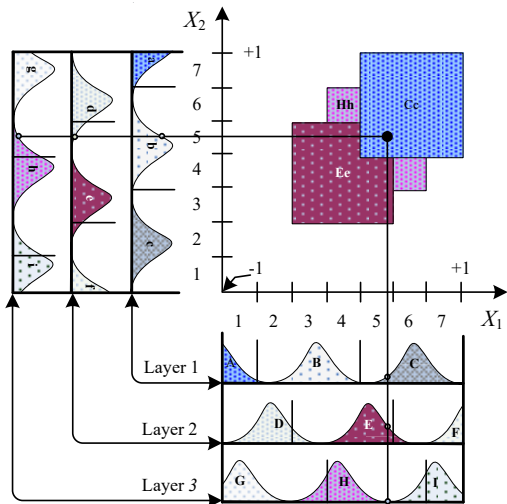


Fig. 3. Schematic of 2-D FCMAC

3) *Receptive-Field Space R*: The information associated with each  $k$ th block and each  $j$ th layer is related to positions in receptive field space. Receptive spatial regions are formed by hypercubes, where each hypercube has multiple inputs. The information in Fig. 3 is presented as follows:

$$b_{jk} = \prod_{i=1}^{n_i} \mu_{ijk}(s_i) = \exp \left[ \sum_{i=1}^{n_i} \frac{-(s_i - m_{ijk})^2}{\sigma_{ijk}^2} \right] \quad (22)$$

For  $i = 1, 2, \dots, n_i, j = 1, 2, \dots, n_j, k = 1, 2, \dots, n_k$ .

Multidimensional receptive fields can be represented as vectors as follows:

$$T = [b_1 \dots b_2 \dots b_{n_k}]^T \in R^{n_k}$$

4) *Weight memory space W*: In this layer, each position of  $T$  adjusts to a specific value denoted by:

$$W = [w_{11} \dots w_{1k} \dots w_{j1} \dots w_{jk}] \quad (23)$$

5) *Output space O*: The output of FCMAC is the sum of the weights, each multiplied by the superblock's corresponding activation value. The mathematical representation of the output can be described as follows:

$$O = \sum_{j=1}^{n_j} \sum_{k=1}^{n_k} W_{jk} \prod_{i=1}^{n_i} \mu_{ijk} \quad (24)$$

For  $i = 1, 2, \dots, n_i, j = 1, 2, \dots, n_j, k = 1, 2, \dots, n_k$ .

### B. The Online Learning Rules

FCMAC is described as in formula (24), in which the adaptation laws of FCMAC are designed as in formulas (25), (27), (28), and the robust controller is designed as in formula (26).

1) *The update rule for the weight layer is derived as follows:*

$$\hat{W} = -\hat{\eta}_w Ts(\underline{e}) \quad (25)$$

$$\tau_{RC} = (2R^2)^{-1} [(I + H^2)R^2 + I] s^T(\underline{e}) \quad (26)$$

Where  $R = \text{diag}[\zeta_1, \zeta_2]$  is the learning rate of the robust controller for the system to converge;  $\hat{\eta}_w$  is positive learning rate for the output weight memory  $w_{jk}$ .

2) *The law for updating the parameters in the Gauss function is given as follows:*

$$\hat{m}_{ijk} = \hat{\eta}_m s(t) \hat{w}_{ijk} \quad (27)$$

$$\hat{\sigma}_{ijk} = \hat{\eta}_\sigma s(t) \hat{w}_{ijk} \quad (28)$$

Where  $\hat{\eta}_m, \hat{\eta}_\sigma$  are positive learning rates for the translation  $\hat{m}_{ijk}$  and dilation  $\hat{\sigma}_{ijk}$ .

## IV. CONTROL SYSTEM STRUCTURE

Fig. 4 depicts an overview of the adaptive FCMAC scheme, which includes three parts: signed distance, FCMAC controller, and robust controller. suppose there exists an optimal  $u_{FCMAC}^*$  to estimate  $\tau_{IDEAL}$  with a robust controller:

$$\tau_{IDEAL} = \tau_{FCMAC}^* + \varepsilon = W^{*T}T + \varepsilon \quad (29)$$

However, in practice such ideal parameters are not available. Therefore, another proposal is made by approximating the output:

$$\tau_{controller} = \tau_{FCMAC} + \tau_{RC} = \hat{W}^T T + \tau_{RC} \quad (30)$$

The Lyapunov function of this structure has the form:

$$L(s(\underline{e}), \tilde{W}) = \frac{1}{2} s^T(\underline{e}) M s(\underline{e}) + \frac{1}{2} \text{tr}[\tilde{W}^T \hat{\eta}_w^{-1} \tilde{W}] \quad (31)$$

Set  $\tilde{W} = W^* - \hat{W}$ , apply equations (17), (18), (29), (30) and derivatives (26), (27):

$$\begin{aligned}
L(s(\underline{e}), \tilde{W}) &= s^T(\underline{e})M\dot{s}(\underline{e}) + tr[\tilde{W}^T \dot{\hat{\eta}}_W^{-1} \dot{\hat{W}}] \quad (32) \\
&= s^T(\underline{e})M \left\{ M^{-1}[\tau_{IDEAL} - \tau_{controller}] - \rho sgn[s(\underline{e}(t))] \right\} \\
&\quad + tr[\tilde{W}^T \dot{\hat{\eta}}_W^{-1} \dot{\hat{W}}] \\
&= s^T(\underline{e})M \left\{ M^{-1}[W^{*T}T + \varepsilon - \tilde{W}^T T - \tau_{RC}] - \rho sgn[s(\underline{e}(t))] \right\} \\
&\quad + tr[\tilde{W}^T \dot{\hat{\eta}}_W^{-1} \dot{\hat{W}}] \\
&= s^T(\underline{e})M \left\{ M^{-1}[\tilde{W}^T T + \varepsilon - \tau_{RC}] - \rho sgn[s(\underline{e}(t))] \right\} \\
&\quad + tr[\tilde{W}^T \dot{\hat{\eta}}_W^{-1} \dot{\hat{W}}] \\
&= s^T(\underline{e})\tilde{W}^T T - tr[\tilde{W}^T \dot{\hat{\eta}}_W^{-1} \dot{\hat{W}}] + s^T(\underline{e})(\varepsilon - \tau_{RC}) - s^T(\underline{e}) \cdot M \\
&\quad \cdot \rho sgn[s(\underline{e}(t))] \\
&\leq s^T(\underline{e})(\varepsilon - \tau_{RC}) \\
&= -\frac{1}{2}s^T(\underline{e})s(\underline{e}) - \frac{1}{2} \left[ \frac{s(\underline{e})}{\lambda} - \lambda_\varepsilon \right]^T \left[ \frac{s(\underline{e})}{\lambda} - \lambda_\varepsilon \right] \\
&\leq -\frac{1}{2}s^T(\underline{e})s(\underline{e}) + \frac{1}{2}\lambda^2 \varepsilon^T \varepsilon \quad (33)
\end{aligned}$$

Integrating equation (33) from  $t = 0$  to  $t = T$ :

$$L(T) - L(0) \leq -\frac{1}{2}\sum_{i=1}^m \int_0^T s_i^2(t) dt + \frac{1}{2}\sum_{k=1}^m \lambda_k^2 \int_0^T \varepsilon_k^2(t) dt \quad (34)$$

The system will completely reach steady state when:

$$\frac{1}{2}\sum_{i=1}^m \int_0^T s_i^2(t) dt \leq L(0) + \frac{1}{2}\sum_{k=1}^m \lambda_k^2 \int_0^T \varepsilon_k^2(t) dt = \frac{1}{2}s^T(\underline{e}(0))Ms(\underline{e}(0)) + \frac{1}{2}tr[\tilde{W}^T(0)\dot{\hat{\eta}}_W^{-1}\tilde{W}(0)] \quad (35)$$

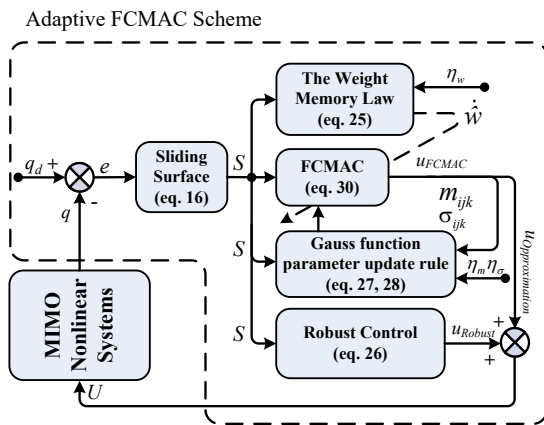


Fig. 4. Structure diagram of FCMAC control system

## V. EXPERIMENT

In this Section, we use a five-bar parallel robot platform to verify and compare the proposed approach to others. This selection stems from the inherent complexity of the mechanical structure of the system, making it challenging to establish an accurate mathematical model. During operation, the interactions among the joints introduce numerous uncertain parameters that cannot be precisely determined. Additionally, various parameters such as viscosity and friction coefficients undergo changes throughout operation, further complicating control efforts. Furthermore, the Fuzzy Cerebellar Model Articulation Controller (FCMAC) network structure, as outlined in part IV, is specifically tailored to accommodate such complexities. This network is designed to handle the uncertainties inherent in the system, providing

adaptability to dynamic changes during operation. The mathematical model described in part II, comprising equations (9)-(15) and detailed parameters in Table I, serves as the foundation for understanding the system dynamics and for the subsequent application and validation of the FCMAC controller on the chosen robot platform.

Table II talks about the network structure parameters when performing simulation experiments.

TABLE I. MODEL PARAMETERS WHEN SIMULATION

Symbol	Parameters
$L_1, L_2, L_3, L_4, L_5$	0.127m
$m_1, m_2, m_3, m_4$	0.065kg
$B_m$	[1,1]
$\delta_1, \delta_2, \delta_3, \delta_4$	1

TABLE II. FCMAC NETWORK STRUCTURAL PARAMETERS

Symbol	Parameters
$n_k$	5
$n_j$	11
$\hat{\eta}_w, \hat{\eta}_m, \hat{\eta}_\sigma$	0.5
$m$	(-1 1)
$\sigma$	0.6

Fig. 5 depicts a robot system consisting of main components such as motors, joints, and encoders. The NI PCIe-6351 board was integrated into the computer to perform experiments and collect data, supporting Simulink on Matlab to control the robot arm. In this installation, the Fuzzy Cerebellar Model Articulation Controller (FCMAC) is the control system used. FCMAC was implemented to optimize the control performance of the robot arm, especially through learning from actual data. This optimization process allows FCMAC to adapt to changing conditions and requirements. The experiment evaluates important factors such as accuracy and mean square error. These metrics are intended to demonstrate the superiority of FCMAC over traditional control methods such as PID and RBF for Quanser's 2-DOF robot system, as depicted in Fig. 6. Expected results from This experiment will provide insight into the quality of FCMAC compared to other traditional methods, such as PID and RBF. The expected results from this test will demonstrate the quality of FCMAC compared to methods such as PID and RBF.

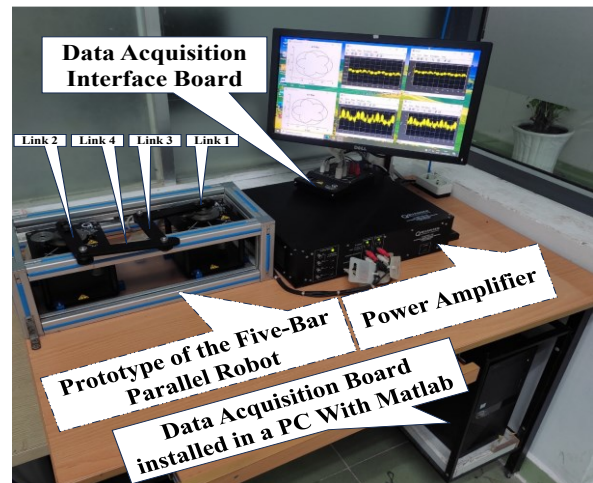


Fig. 5. Experimental system



Fig. 6. Quanser's 2 DOF Robot model

**A. Experimental Results in the Absence of Uncertain Components**

Fig. 7 shows the difference between the actual position and the reference position of the robot joints. It is easy to see that FCMAC can stabilize and maintain a good position with the reference orbit. The RBF and PID algorithms are still capable of maintaining location and processing but are less efficient than FCMAC.

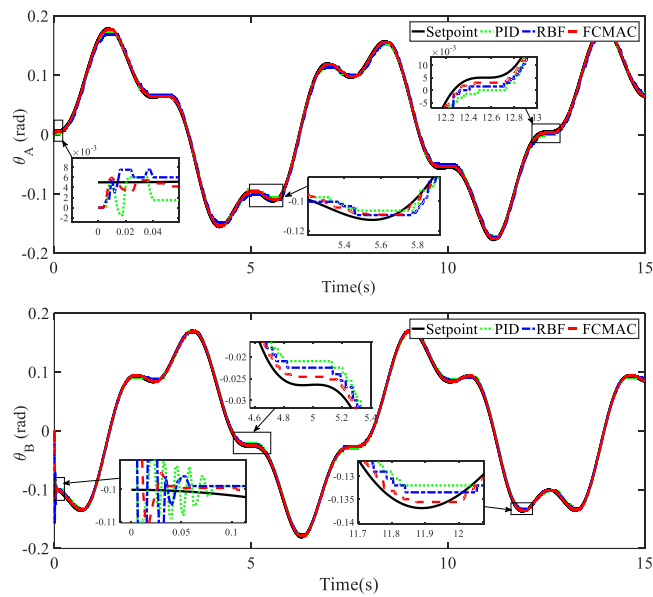


Fig. 7. Actual position relative to the robot's  $\theta_A$  and  $\theta_B$  reference positions

Fig. 8 shows the error used to evaluate the accuracy. The error reduction and stability of FCMAC compared to RBF and PID are a testament to its excellent performance in maintaining positions close to the reference position.

Fig. 9 depicts the difference between the actual trajectory and the reference trajectory on the system, showing that FCMAC outperforms RBF and PID regarding trajectory tracking ability. Demonstrates the flexibility and high adaptability of the FCMAC algorithm.

Table III depicts the performance of three different methods, FCMAC, RBF, and PID, without uncertainty components. For  $e_A$ , PID has the most significant value (6.18e-03), followed by RBF (5.77e-03) and FCMAC (2.24e-03). When considering  $mse_A$ , FCMAC continues to have the smallest value (1.160e-04), indicating the highest accuracy among the three methods. In the case of  $e_B$  and  $mse_B$ , FCMAC continues to have the smallest value. Shows higher accuracy compared to RBF and PID. In short, in the absence of uncertainty, FCMAC maintains good stability and accuracy.

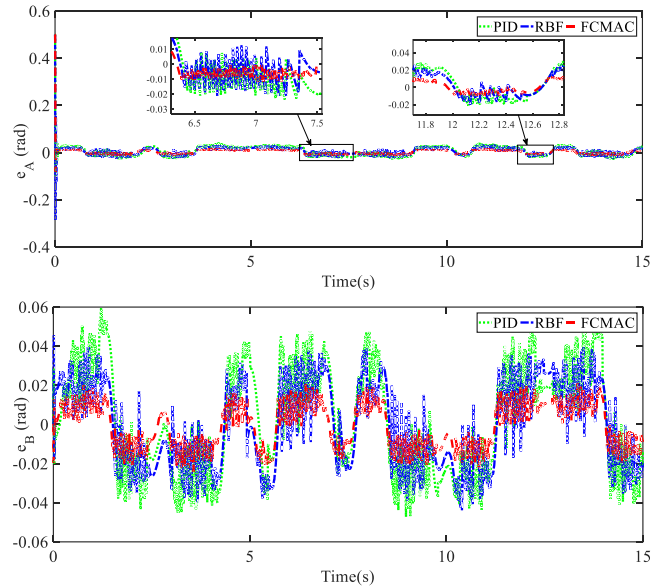


Fig. 8.  $\theta_A$  and  $\theta_B$  error of the robot system during actual operation

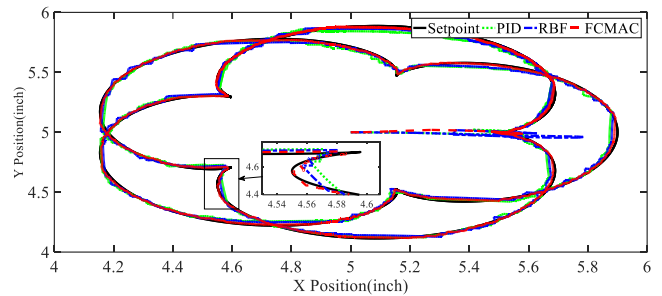


Fig. 9. Actual trajectory compared to reference trajectory when the robot system is in actual operation

TABLE III. THE ACTUAL OPERATION DATA SHEET DOES NOT INCLUDE ANY UNCERTAIN COMPONENTS

Symbol	FCMAC	RBF	PID
$e_A$	2.24e-03	5.77e-03	6.18e-03
$mse_A$	1.160e-04	6.85e-04	3.04e-03
$e_B$	-8.15e-04	-2.05e-03	3.68e-03
$mse_B$	5.78e-03	1.51e-02	3.83e-02

**B. Experimental Results in Case of Inclusion of Uncertain Component**

In actual systems, uncertainty can arise from many different sources. Adding uncertainty components is necessary to evaluate the capabilities of the proposed FCMAC structure. Below is the definition of the uncertainty components added at time  $t = 4s$ :

$$L(\mathbf{x}, t) = t_l + f_l$$

Where  $t_l = [0.05 * \cos(t) * \text{sign}(q_1 * q_2); -0.01 * \sin(t)]$  and  $f_l = [0.01 * \cos(t); -0.05 * \cos(t) * \text{sign}(q_1 * q_2)]$ .

Fig. 10 depicts the difference between the actual position and the reference position of the robot joints. FCMAC is stable and maintains well with the reference trajectory at the start. Notably, noise appeared at time  $t=4s$  and caused a significant difference in the system. FCMAC still demonstrates excellence in maintaining system control quality, outperforming other algorithms.

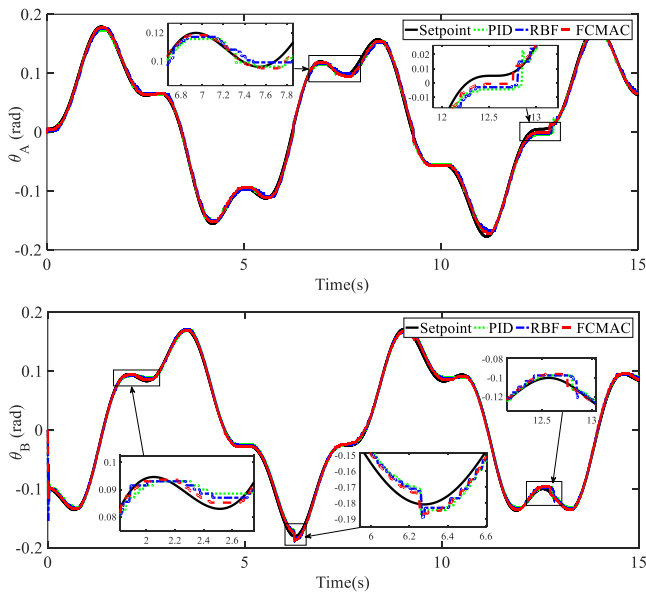


Fig. 10. Actual position relative to the robot's  $\theta_A$  and  $\theta_B$  reference positions

Fig. 11 shows the fluctuation resistance of the control algorithm. FCMAC demonstrates the precise control and anti-uncertainty component ability of FCMAC in the actual environment at time  $t = 4s$ .

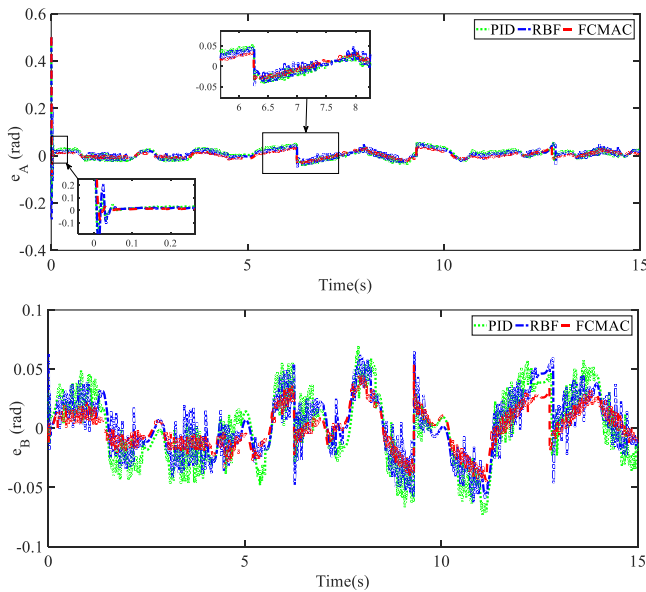


Fig. 11.  $\theta_A$  and  $\theta_B$  error of the robot system during actual operation

Fig. 12 shows the actual trajectory and reference trajectory on the system. From the figure, FCMAC is superior to RBF and PID in orbit tracking ability. Especially when faced with uncertain components, highlighting the adaptability of the FCMAC algorithm.

Table IV depicts the performance of three methods, FCMAC, RBF, and PID, with uncertainty components. For  $e_A$ , PID has the highest value (8.08e-03), followed by RBF (7.59e-03) and FCMAC (3.66e-03). When considering  $mse_A$ , FCMAC retains the smallest value (1.270e-04), indicating a relatively higher accuracy than RBF and PID. For  $e_B$ , FCMAC (3.88e-04) and RBF (4.01e-04) have smaller values than PID (2.83e-03). FCMAC continues to have the smallest

$mse_B$  value (1.43e-02), followed by RBF (2.01e-02) and PID (4.63e-02). FCMAC maintains good stability and accuracy even when uncertain components exist in the system.

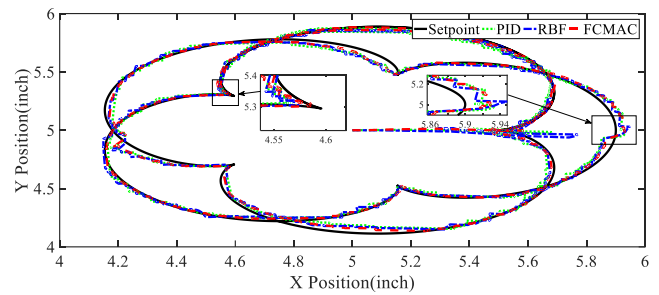


Fig. 12. Actual trajectory compared to reference trajectory when the robot system is in actual operation

TABLE IV. THE ACTUAL OPERATION DATA SHEET INCLUDE UNCERTAIN COMPONENTS

Symbol	FCMAC	RBF	PID
$e_A$	3.66e-03	7.59e-03	8.08e-03
$mse_A$	1.270e-04	7.45e-04	3.24e-03
$e_B$	3.88e-04	4.01e-04	2.83e-03
$mse_B$	1.43e-02	2.01e-02	4.63e-02

### VI. CONCLUSION AND DISCUSSION

This study presents and utilizes the Fuzzy Cerebellar Model Controller (FCMAC) algorithm to control the robot system along a time-based reference trajectory. The unique aspect of this research is the integration of Fuzzy's advantages into CMAC's capabilities to handle nonlinear systems, optimize fuzzy solutions, and manage uncertainties. This method is effective and practical. Lyapunov and robust controllers demonstrate the stability of FCMAC. Experimental results emphasize the benefits of the proposed method. This could be a steppingstone towards other practical applications such as robot control, engine control, UAVs, etc.

However, the drawback of this controller lies in optimizing Gaussian function parameters, network structure learning speed, and robust control. It's noteworthy that FCMAC only addresses one of the two most significant drawbacks of CMAC: the ability to compute input parameters at the Associative Memory Space. The remaining drawback is CMAC's processing and adaptation capabilities with complex nonlinear systems. In the future, research aims to address the remaining shortcomings. It may involve integrating wavelet networks or using Type-2 fuzzy networks to enhance processing capabilities at the Associative Memory Space. Regarding drawbacks, further studies will explore various methods or combine them with Brain Emotion Learning networks to increase the overall integration capability and achieve higher accuracy.

### REFERENCES

- [1] Y. Cao, W. Jiang, and J. Wang, "Anti-synchronization of delayed memristive neural networks with leakage term and reaction-diffusion terms," *Knowledge-Based Systems*, vol. 233, p. 107539, 2021.
- [2] F. Chao, D. Zhou, C. -M. Lin, L. Yang, C. Zhou, and C. Shang, "Type-2 Fuzzy Hybrid Controller Network for Robotic Systems," in *IEEE Transactions on Cybernetics*, vol. 50, no. 8, pp. 3778-3792, Aug. 2020, doi: 10.1109/TCYB.2019.2919128.
- [3] C.-F. Hsu, B.-R. Chen, and B.-F. Wu, "Broad-learning recurrent Hermite neural control for unknown nonlinear systems," *Knowledge-Based Systems*, vol. 242, p. 108263, 2022.

- [4] B. Ma, Y. Li, T. An, and B. Dong, "Compensator-critic structure-based neurooptimal control of modular robot manipulators with uncertain environmental contacts using non-zero-sum games," *Knowledge-Based Systems*, vol. 224, p. 107100, 2021.
- [5] L. Wang, K. Zeng, C. Hu, and Y. Zhou, "Multiple finite-time synchronization of delayed inertial neural networks via a unified control scheme," *Knowledge-Based Systems*, vol. 236, p. 107785, 2022.
- [6] Y. Wang, J. Sun, H. He, and C. Sun, "Deterministic Policy Gradient With Integral Compensator for Robust Quadrotor Control," in *IEEE Transactions on Systems, Man, and Cybernetics: Systems*, vol. 50, no. 10, pp. 3713-3725, Oct. 2020, doi: 10.1109/TSMC.2018.2884725.
- [7] J. Xiao, Y. Li, and S. Wen, "Mittag-Leffler synchronization and stability analysis for neural networks in the fractional-order multidimension field," *Knowledge-Based Systems*, vol. 231, p. 107404, 2021.
- [8] Y. Yue, H. Yang, F. Liu, and H. Zang, "Cooperative control for multiple quadrotors under position deviations and aerodynamic drag," *Mechanical Systems and Signal Processing*, vol. 147, p. 107096, 2021.
- [9] J. Y. Lau, W. Liang, and K. K. Tan, "Motion Control for Piezoelectric-Actuator-Based Surgical Device Using Neural Network and Extended State Observer," in *IEEE Transactions on Industrial Electronics*, vol. 67, no. 1, pp. 402-412, Jan. 2020, doi: 10.1109/TIE.2019.2897542.
- [10] G. Tao, S. Chen, X. Tang, and S. M. Joshi, "Adaptive control of systems with actuator failures," *Springer Science & Business Media*, 2013.
- [11] X. Zhang, J. Ma, Z. Cheng, S. Huang, S. S. Ge, and T. H. Lee, "Trajectory Generation by Chance-Constrained Nonlinear MPC With Probabilistic Prediction," in *IEEE Transactions on Cybernetics*, vol. 51, no. 7, pp. 3616-3629, 2021, doi: 10.1109/TCYB.2020.3032711.
- [12] L. Kong and J. Yuan, "Disturbance-observer-based fuzzy model predictive control for nonlinear processes with disturbances and input constraints," *ISA Transactions*, vol. 90, pp. 74-88, 2019.
- [13] W. Gu, J. Yao, Z. Yao, and J. Zheng, "Output feedback model predictive control of hydraulic systems with disturbances compensation," *ISA Transactions*, vol. 88, pp. 216-24, 2019.
- [14] J. Ma, Z. Cheng, X. Zhang, M. Tomizuka, and T. H. Lee, "Optimal Decentralized Control for Uncertain Systems by Symmetric Gauss-Seidel Semi-Proximal ALM," in *IEEE Transactions on Automatic Control*, vol. 66, no. 11, pp. 5554-5560, Nov. 2021, doi: 10.1109/TAC.2021.3052768.
- [15] W. Liang, S. Huang, S. Chen, and K. K. Tan, "Force estimation and failure detection based on disturbance observer for an ear surgical device," *ISA Transactions*, vol. 66, pp. 476-84, 2017.
- [16] J. Ma, S. L. Chen, C. S. Teo, A. Tay, A. Al Mamun, and K. K. Tan, "Parameter space optimization towards integrated mechatronic design for uncertain systems with generalized feedback constraints," *Automatica*, vol. 105, pp. 149-58, 2019.
- [17] J. Ma, Z. Cheng, H. Zhu, X. Li, M. Tomizuka, and T. H. Lee, "Convex Parameterization and Optimization for Robust Tracking of a Magnetically Levitated Planar Positioning System," in *IEEE Transactions on Industrial Electronics*, vol. 69, no. 4, pp. 3798-3809, April 2022, doi: 10.1109/TIE.2021.3070518.
- [18] X. Zhang, W. Jiang, Z. Li, and S. Song, "A hierarchical Lyapunov-based cascade adaptive control scheme for lower-limb exoskeleton," *European Journal of Control*, vol. 50, pp. 198-208, 2019.
- [19] C. Shen, Y. Shi, and B. Buckham, "Trajectory Tracking Control of an Autonomous Underwater Vehicle Using Lyapunov-Based Model Predictive Control," in *IEEE Transactions on Industrial Electronics*, vol. 65, no. 7, pp. 5796-5805, July 2018, doi: 10.1109/TIE.2017.2779442.
- [20] Y. Wang, J. Chen, F. Yan, K. Zhu, and B. Chen, "Adaptive super-twisting fractional-order nonsingular terminal sliding mode control of cable-driven manipulators," *ISA Trans.*, vol. 86, pp. 163-180, 2019.
- [21] J. Y. Lau, W. Liang, and K. K. Tan, "Adaptive sliding mode enhanced disturbance observer-based control of surgical device," *ISA Transactions*, vol. 90, pp. 178-188, 2019.
- [22] W. Fang *et al.*, "Visual-Guided Robotic Object Grasping Using Dual Neural Network Controllers," in *IEEE Transactions on Industrial Informatics*, vol. 17, no. 3, pp. 2282-2291, March 2021, doi: 10.1109/TII.2020.2995142.
- [23] X. Guan, J. Hu, J. Qi, D. Chen, F. Zhang, and G. Yang, "Observer-based sliding mode control for networked systems subject to communication channel fading and randomly varying nonlinearities," *Neurocomputing*, vol. 437, pp. 312-324, 2021.
- [24] S. He, Y. Xu, Y. Wu, Y. Li, and W. Zhong, "Adaptive consensus tracking of multirobotic systems via using integral sliding mode control," *Neurocomputing*, vol. 455, pp. 154-162, 2021.
- [25] Y. Ren, W. Zhou, Z. Li, L. Liu, and Y. Sun, "Prescribed-time leader-following consensus for stochastic second-order multi-agent systems subject to actuator failures via sliding mode control strategy," *Neurocomputing*, vol. 425, pp. 82-95, 2021.
- [26] W. Wang, X. Jia, Z. Wang, X. Luo, L. Li, J. Kurths, and M. Yuan, "Fixed-time synchronization of fractional order memristive MAM neural networks by sliding mode control," *Neurocomputing*, vol. 401, pp. 364-376, 2020.
- [27] W. Ji, J. Qiu, and H. R. Karimi, "Fuzzy-Model-Based Output Feedback Sliding-Mode Control for Discrete-Time Uncertain Nonlinear Systems," in *IEEE Transactions on Fuzzy Systems*, vol. 28, no. 8, pp. 1519-1530, Aug. 2020, doi: 10.1109/TFUZZ.2019.2917127.
- [28] T. Q. Ngo, T. H. Tran, T. T. H. Le, and B. M. Lam, "An Application of Modified T2FHC Algorithm in Two-Link Robot Controller," *Journal of Robotics and Control (JRC)*, vol. 4, no. 4, Aug. 2023.
- [29] X. Li, Z. Zhu, N. Shen, W. Dai, and Y. Hu, "Deeply feature learning by CMAC network for manipulating rehabilitation robots," *Future Generation Computer Systems*, vol. 121, pp. 19-24, 2021.
- [30] N. Tan, C. Li, P. Yu, and F. Ni, "Two model-free schemes for solving kinematic tracking control of redundant manipulators using CMAC networks," *Applied Soft Computing*, vol. 126, p. 109267, 2022.
- [31] E. Stingu and F. L. Lewis, "An approximate Dynamic Programming based controller for an underactuated 6DoF quadrotor," *2011 IEEE Symposium on Adaptive Dynamic Programming and Reinforcement Learning (ADPRL)*, pp. 271-278, 2011, doi: 10.1109/ADPRL.2011.5967394.
- [32] Z. Zhong, H. -K. Lam, H. Ying, and G. Xu, "CMAC-Based SMC for Uncertain Descriptor Systems Using Reachable Set Learning," in *IEEE Transactions on Systems, Man, and Cybernetics: Systems*, vol. 54, no. 2, pp. 693-703, Feb. 2024.
- [33] T. Q. Ngo, M. K. Duong, D. C. Pham, and D.-N. Nguyen, "Adaptive Wavelet CMAC Tracking Control for Induction Servomotor Drive System," *Journal of Electrical Engineering & Technology*, vol. 14, no. 1, pp. 209-218, 2019.
- [34] T. -T. Huynh *et al.*, "A New Self-Organizing Fuzzy Cerebellar Model Articulation Controller for Uncertain Nonlinear Systems Using Overlapped Gaussian Membership Functions," in *IEEE Transactions on Industrial Electronics*, vol. 67, no. 11, pp. 9671-9682, Nov. 2020.
- [35] T. Q. Ngo, D. K. Hoang, T. T. Tran, T. T. Nguyen, V. T. Nguyen, and L. H. Le, "A Novel Self-Organizing Fuzzy Cerebellar Model Articulation Controller Based Overlapping Gaussian Membership Function for Controlling Robotic System," *International Journal Of Computers Communications & Control*, vol. 17, no. 4, 4606, 2022.
- [36] T. Q. Ngo, T. T. H. Le, B. M. Lam, and T. K. Pham, "Adaptive Single-Input Recurrent WCMAC-Based Supervisory Control for De-icing Robot Manipulator," *Journal of Robotics and Control (JRC)*, vol. 4, no. 4, July 2023.
- [37] Z. Piao, C. Guo, and S. Sun, "Adaptive Backstepping Sliding Mode Dynamic Positioning System for Pod Driven Unmanned Surface Vessel Based on Cerebellar Model Articulation Controller," in *IEEE Access*, vol. 8, pp. 48314-48324, 2020.
- [38] H. Wu, H. An, Q. Wei, and H. Ma, "Fuzzy CMAC-Based Adaptive Scale Force Control of Body Weight Support Exoskeletons," in *IEEE Access*, vol. 8, pp. 147286-147294, 2020.
- [39] C. Dong, Z. Yu, X. Chen, H. Chen, Y. Huang, and Q. Huang, "Adaptability Control Towards Complex Ground Based on Fuzzy Logic for Humanoid Robots," in *IEEE Transactions on Fuzzy Systems*, vol. 30, no. 6, pp. 1574-1584, June 2022.
- [40] C. -F. Juang, C. -H. Lu, and C. -A. Huang, "Navigation of Three Cooperative Object-Transportation Robots Using a Multistage Evolutionary Fuzzy Control Approach," in *IEEE Transactions on Cybernetics*, vol. 52, no. 5, pp. 3606-3619, May 2022.
- [41] N. Tan, Z. Ye, P. Yu, and F. Ni, "A Dual Fuzzy-Enhanced Neurodynamic Scheme for Model-Less Kinematic Control of

- Redundant and Hyperredundant Robots,” in *IEEE Transactions on Fuzzy Systems*, vol. 30, no. 10, pp. 4409-4422, Oct. 2022.
- [42] S. Xu and B. He, “Robust Adaptive Fuzzy Fault Tolerant Control of Robot Manipulators With Unknown Parameters,” in *IEEE Transactions on Fuzzy Systems*, vol. 31, no. 9, pp. 3081-3092, Sept. 2023.
- [43] Q. Lin, X. Chen, C. Chen, and J. M. Garibaldi, “A Novel Quality Control Algorithm for Medical Image Segmentation Based on Fuzzy Uncertainty,” in *IEEE Transactions on Fuzzy Systems*, vol. 31, no. 8, pp. 2532-2544, Aug. 2023, doi: 10.1109/TFUZZ.2022.3228332.
- [44] Y. Ren, Z. Zhao, C. K. Ahn, and H. -X. Li, “Adaptive Fuzzy Control for an Uncertain Axially Moving Slung-Load Cable System of a Hovering Helicopter With Actuator Fault,” in *IEEE Transactions on Fuzzy Systems*, vol. 30, no. 11, pp. 4915-4925, Nov. 2022, doi: 10.1109/TFUZZ.2022.3164512.
- [45] B. Zhu, Y. Wang, H. Zhang, and X. Xie, “Fuzzy Functional Observer-Based Finite-Time Adaptive Sliding-Mode Control for Nonlinear Systems With Matched Uncertainties,” in *IEEE Transactions on Fuzzy Systems*, vol. 30, no. 4, pp. 918-932, April 2022, doi: 10.1109/TFUZZ.2021.3050846.
- [46] W. Zhao, Y. Liu, and X. Yao, “Adaptive Fuzzy Containment and Vibration Control for Multiple Flexible Manipulators With Model Uncertainties,” in *IEEE Transactions on Fuzzy Systems*, vol. 31, no. 4, pp. 1315-1326, April 2023, doi: 10.1109/TFUZZ.2022.3199573.
- [47] F. Ardilla, M. I. Mas’udi, and I. K. Wibowo, “Fusion of Feedforward and Feedback Control Using Fuzzy for Active Handling and Dribbling System in MSL Robot Soccer,” *International Journal on Advance Science, Engineering and Information Technology*, vol. 9, no. 6, pp. 1950-1958, 2019.
- [48] S. Wang, “Mobile Robot Path Planning based on Fuzzy Logic Algorithm in Dynamic Environment,” *2022 International Conference on Artificial Intelligence in Everything (AIE)*, pp. 106-110, 2022, doi: 10.1109/AIE57029.2022.00027.
- [49] I. Reguii, I. Hassani, and C. Rekik, “Neuro-fuzzy Control of a Mobile Robot,” *2022 IEEE 21st international Cnference on Sciences and Techniques of Automatic Control and Computer Engineering (STA)*, pp. 45-50, 2022, doi: 10.1109/STA56120.2022.10018999.
- [50] S. Hanana, N. Krichen, and M. S. Masmoudi, “Dual Fuzzy Logic Controllers for Omnidirectional Robot Navigation and Obstacle Avoidance,” *2022 IEEE 21st international Cnference on Sciences and Techniques of Automatic Control and Computer Engineering (STA)*, pp. 100-105, 2022, doi: 10.1109/STA56120.2022.10019080.
- [51] R. K. Ikbar, E. Mulyana, R. Mardiati, and R. R. Nurmalsari, “Fire Fighting Robot Using Flame Detector and Ultrasonic Based on Fuzzy Logic Control,” *2022 16th International Conference on Telecommunication Systems, Services, and Applications (TSSA)*, pp. 1-6, 2022, doi: 10.1109/TSSA56819.2022.10063922.
- [52] C. -M. Lin, M. -S. Yang, F. Chao, X. -M. Hu, and J. Zhang, “Adaptive Filter Design Using Type-2 Fuzzy Cerebellar Model Articulation Controller,” in *IEEE Transactions on Neural Networks and Learning Systems*, vol. 27, no. 10, pp. 2084-2094, Oct. 2016, doi: 10.1109/TNNLS.2015.2491305.
- [53] W. Fang *et al.*, “A recurrent emotional CMAC neural network controller for vision-based mobile robots,” *Neurocomputing*, vol. 334, pp. 227-238, Mar. 2019.
- [54] C. Lin, Y. Liu, and H. Li, “SoPC-based function-link cerebellar model articulation control system design for magnetic ball levitation systems,” *IEEE Trans. Ind. Electron.*, vol. 61, no. 8, pp. 4265-4273, Aug. 2014.
- [55] H. Ying, F. Lin, and R. Sherwin, “Fuzzy discrete event systems with gradient-based online learning,” in *Proc. FUZZ-IEEE Conf.*, pp. 1-6, 2019.
- [56] C. Lin, R. Ramarao, and S. Gopalai, “Self-organizing adaptive fuzzy brain emotional learning control for nonlinear systems,” *Int. J. Fuzzy Syst.*, vol. 21, no. 7, pp. 1989-2007, 2019.
- [57] X. Jing and L. Cheng, “An optimal PID control algorithm for training feedforward neural networks,” *IEEE Trans. Ind. Electron.*, vol. 60, no. 6, pp. 2273-2283, Jun. 2013.
- [58] C. C. Jou, “A fuzzy cerebellar model articulation controller,” *1992 Proceedings, IEEE International Conference on Fuzzy Systems*, pp. 1171-1178, 1992, doi: 10.1109/FUZZY.1992.258722.
- [59] J. Guan, C. -M. Lin, G. -L. Ji, L. -W. Qian, and Y. -M. Zheng, “Robust Adaptive Tracking Control for Manipulators Based on a TSK Fuzzy Cerebellar Model Articulation Controller,” in *IEEE Access*, vol. 6, pp. 1670-1679, 2018, doi: 10.1109/ACCESS.2017.2779940.
- [60] A. Mohammadzadeh and S. Ghaemi, “Optimal synchronization of fractional-order chaotic systems subject to unknown fractional order, input nonlinearities and uncertain dynamic using type-2 fuzzy CMAC,” *Nonlinear Dynam.*, vol. 88, pp. 2993-3002, 2017.
- [61] C.-M. Lin, T.-T. Huynh, and T.-L. Le, “Adaptive TOPSIS fuzzy CMAC backstepping control system design for nonlinear systems,” *Soft Computing*, vol. 23, pp. 6947-66, 2019.
- [62] L. Cheng, Y. Lin, Z. -G. Hou, M. Tan, J. Huang, and W. J. Zhang, “Adaptive Tracking Control of Hybrid Machines: A Closed-Chain Five-Bar Mechanism Case,” in *IEEE/ASME Transactions on Mechatronics*, vol. 16, no. 6, pp. 1155-1163, Dec. 2011.